Published in final edited form as:
Neurobiol Dis. 2013 October ; 58: 192–199. doi:10.1016/j.nbd.2013.06.002.

Enhanced Ca^{2+}-dependent glutamate release from astrocytes of the BACHD Huntington's disease mouse model

William Lee[a], **Reno C. Reyes**[a,1], **Manoj K. Gottipati**[a], **Karon Lewis**[b], **Mathieu Lesort**[c], **Vladimir Parpura**[a,d,*], and **Michelle Gray**[b,*]

[a]Department of Neurobiology, University of Alabama at Birmingham, Birmingham, AL 35294

[b]Department of Neurology and Center for Neurodegeneration and Experimental Therapeutics, University of Alabama at Birmingham, Birmingham, AL 35294

[c]Department of Psychiatry and Behavioral Neurobiology, University of Alabama at Birmingham, Birmingham, AL 35294

[d]Department of Biotechnology, University or Rijeka, 51000 Rijeka, Croatia

Abstract

Huntington's disease (HD) causes preferential loss of a subset of neurons in the brain although the huntingtin protein is expressed broadly in various neural cell types, including astrocytes. Glutamate-mediated excitotoxicity is thought to cause selective neuronal injury, and brain astrocytes have a central role in regulating extracellular glutamate. To determine whether full-length mutant huntingtin expression causes a cell-autonomous phenotype and perturbs astrocyte gliotransmitter release, we studied cultured cortical astrocytes from BACHD mice. Here, we report augmented glutamate release through Ca^{2+}-dependent exocytosis from BACHD astrocytes. Although such release is usually dependent on cytosolic Ca^{2+} levels, surprisingly, we found that BACHD astrocytes displayed Ca^{2+} dynamics comparable to those in wild type astrocytes. These results point to a possible involvement of other factors in regulating Ca^{2+}- dependent/vesicular release of glutamate from astrocytes. We found a biochemical footprint that would lead to increased availability of cytosolic glutamate in BACHD astrocytes: i) augmented *de novo* glutamate synthesis due to an increase in the level of the astrocyte specific mitochondrial enzyme pyruvate carboxylase; and ii) unaltered conversion of glutamate to glutamine, as there were no changes in the expression level of the astrocyte specific enzyme glutamine synthetase. This work identifies a new mechanism in astrocytes that could lead to increased levels of extracellular glutamate in HD and thus may contribute to excitotoxicity in this devastating disease.

Keywords

Huntington's Disease; Astrocytes; Glutamate; Pyruvate carboxylase

*Corresponding author during submission and publication: University of Alabama at Birmingham 1720 2nd Ave S CIRC 525B1 Birmingham, AL 35294 205-996-4748 mccgray@uab.edu. *Corresponding author publication: University of Alabama at Birmingham 1719 6th Avenue South, CIRC 429 Birmingham, AL 35294 vlad@uab.edu.
[1]**Present Address:** Department of Neurology, University of California, San Francisco and Veterans Affairs Medical Center, San Francisco, CA 94121

Introduction

Huntington's disease (HD) is an autosomal dominant, progressive and fatal neurodegenerative disorder caused by a CAG repeat expansion in the gene encoding the widely expressed protein huntingtin (htt) (Group, 1993; Sharp et al., 1995; Singhrao et al., 1998). Neurodegeneration is most prominent in striatal medium spiny neurons (MSNs) and to a lesser extent in cortical pyramidal neurons (Hedreen et al., 1991; Vonsattel et al., 1985). Expression of mutant htt (mhtt) is necessary in multiple neural cell types to recapitulate key features of HD. When expression is limited to only pyramidal neurons in the cortex or MSNs in the striatum in mice, no significant neurodegenerative changes occur (Gu et al., 2007; Gu et al., 2005). Thus, various cell types are likely key for the development of HD phenotypes.

One major hypothesis in HD is excitotoxicity caused principally by excessive activation of the N-methyl-D-aspartate (NMDARs) receptors (Fan and Raymond, 2007). There is extensive glutamatergic input to the striatum and cortex, with high densities of NMDARs on MSNs (Albin et al., 1992; Landwehrmeyer et al., 1995). Intrastriatal injections of NMDAR agonists in primates and mice lead to degeneration and morphological changes in MSNs resembling HD patient pathology (Beal et al., 1986).

The htt protein is present in astrocytes (Singhrao et al., 1998) and evidence exists for altered astrocyte function in HD (Faideau et al., 2010; Vonsattel and DiFiglia, 1998). In the R6/2 model, there is defective astrocytic glutamate uptake (Behrens et al., 2002; Lievens et al., 2001), and associated increases in extracellular glutamate in the striatum (Arzberger et al., 1997; Hassel et al., 2008). Astrocytes from R6/2 mice increase neuronal vulnerability to toxicity, while wild type (WT) astrocytes protect mhtt expressing neurons against toxicity (Shin et al., 2005).

Astrocyte function is central to regulation of extracellular glutamate. Astrocytes are the only cells in the brain that can synthesize glutamate *de novo* (Hertz et al., 1999). They release glutamate using various mechanisms, including Ca^{2+}-dependent vesicular exocytosis (Parpura and Zorec, 2010). Glutamate released from astrocytes can act on neuronal glutamate receptors (Araque et al., 1999) and activate extrasynaptic NMDARs to modulate neuronal excitability and synaptic transmission (Fellin et al., 2004). Astrocytes are the main site of glutamate uptake, principally through the plasma membrane glutamate transporter EAAT2/GLT-1 (Maragakis and Rothstein, 2001); impairment of astrocytic glutamate uptake can contribute to excitotoxicity (Maragakis and Rothstein, 2001).

To determine what impact fl-mhtt has on astrocyte function in gliotransmission we used the BACHD mouse model of HD (Gray et al., 2008; Menalled et al., 2009). The BACHD mouse model contains full-length human mutant huntingtin (fl-mhtt) with 97 polyglutamines encoded by a modified huntingtin transgene on a human Bacterial Artificial Chromosome (BAC). The fl-mhtt protein is expressed throughout the brain of the BACHD mice. These mice exhibit accumulation of mhtt positive aggregates in the brain and atrophy of the cortex and striatum. BACHD mice also show progressive motor and psychiatric-like behavioral phenotypes (Gray et al., 2008; Menalled et al., 2009). In the present study we have identified augmented Ca^{2+}-dependent exocytotic release of glutamate into the extracellular space of cortical astrocytes from BACHD mice. This release enhancement cannot be explained by Ca^{2+} dynamics. Rather surprisingly, the enhancement in release is due to an increased availability of cytosolic glutamate for vesicular packaging, owing to increased expression of the critical enzyme for glutamate *de novo* synthesis pyruvate carboxylase in BACHD astrocytes. Thus, these data demonstrate a novel mechanism whereby fl-mhtt cell-

autonomously affects the function of astrocytes and produces enhanced glutamate release that likely contributes to glutamate excitotoxicity and neural circuit dysfunction.

Materials & Methods

Astrocyte cultures

All animal procedures were performed in accordance with the National Institutes of Health Guide for the Care and Use of Laboratory Animals and were approved by the University of Alabama at Birmingham Institutional Care and Use Committee. BACHD mice (Gray et al., 2008) were maintained by breeding with the “wild type” (WT), i.e. background strain mice (FvB/N, The Jackson Laboratory). We used 1-to 2-day-old BACHD and WT mice to obtain purified cortical astrocyte culture (>99%) grown in flasks and on polyethyleneimine (PEI, 1mg/ml)-coated coverslips, as we previously described (Reyes et al., 2011). At least three independent cultures were used for imaging data collection and analysis. Imaging experiments were done at room temperature (RT) (20-24°C).

Immunocytochemistry

Labeling of astrocytes using indirect immunocytochemistry (ICC) for glial fibrillary acidic protein (GFAP) was done as previously described (Gottipati et al., 2012; Montana et al., 2004). Briefly, astrocytes on glass coverslips were fixed with freshly prepared Dent’s fixative [80% methanol and 20% dimethyl sulfoxide] for 30 minutes and then permeabilized with 0.25% (v/v) Triton X-100 for 10 minutes. To prevent non-specific binding, the cells were incubated with 10% (v/v) goat serum in phosphate buffered saline (PBS) for 30 minutes followed by an overnight (> 12h) incubation of the cells at 4°C with monoclonal primary antibody against GFAP (1:500; MP Biomedicals). Cells were then washed three times with PBS and incubated for 1h with tetramethylrhodamine isothiocyanate (TRITC)-conjugated secondary antibody (1:200; Millipore) at RT. After washing twice with PBS, we colabeled cell nuclei using 4′, 6-diamidino-2-phenylindole dilactate (DAPI dilactate; 3 μM; Molecular Probes) for 5 min at RT diluted in PBS. Finally, after washing twice with water, the coverslips were mounted onto glass microscopic slides in ProLong® Gold antifade reagent (Invitrogen) to prevent photobleaching. Immunoreactivity of GFAP and nuclear stain were visualized using standard TRITC and DAPI filter sets, respectively, under an inverted microscope (Nikon TE300) equipped with wide-field fluorescence illumination (xenon arc lamp; 100W).

Mechanical stimulation

To elicit cytosolic Ca^{2+} increases in solitary astrocytes and subsequent release of glutamate, we employed a glass patch pipette to deliver mechanical stimulus (Hua et al., 2004). The patch pipette was lowered onto solitary astrocytes with a micromanipulator (Narishige, East Meadow, NY). The contact with the plasma membrane, lasting less than 1 sec, which represents the mechanical stimulus, was monitored by measuring the change in pipette resistance using a patch-clamp amplifier (PC-ONE; Dagan, Minneapolis, MN) that delivered −20 mV, 10 ms square pulses at 50 Hz.

Intracellular calcium and extracellular glutamate imaging

Mechanically-induced changes in cytosolic Ca^{2+} levels of cultured solitary astrocytes were measured using the Ca^{2+} indicator fluo-3, while the L-glutamate dehydrogenase (GDH)-linked assay was used to measure extracellular levels of glutamate as previously described (Reyes et al., 2011). Briefly, for Ca^{2+} imaging, astrocytes were loaded with fluo-3 AM (10 μg/ml; Life Technologies Corp. Invitrogen™) in external solution supplemented with pluronic acid (0.025% w/v) for 30 min at RT. External solution (pH 7.35) contained (in

mM): NaCl (140), KCl (5), $CaCl_2$ (2), $MgCl_2$ (2), HEPES (10), and glucose (5). To allow deesterification of fluo-3 AM, cells were subsequently kept in external solution for 30 min at room temperature. Coverslips containing fluo-3 loaded astrocytes were mounted onto a recording chamber. Astrocytes were visualized using a microscope equipped with a standard fluorescein isothiocyanate (FITC) filter set (Chroma Technology, Rockingham, VT, USA). Fluorescence intensities obtained from astrocyte bodies were corrected (digital subtraction) for the background fluorescence measured from regions of coverslips containing no cells. Fluorescence data were expressed as dF/Fo (%) with the cell baseline fluorescence (Fo) representing the average of the first 5 images before mechanical stimulation while dF represents the change in fluorescence emission.

For glutamate imaging, coverslips containing cultured astrocytes were mounted onto a recording chamber filled with external solution. A set of images containing the cell of interest were taken in a sham run to correct for reduction of fluorescence due to photobleaching. In the experimental run, the external solution was exchanged with the fresh external solution additionally containing 1 mM of β-nicotinamide adenine dinucleotide (NAD^+; Sigma) and ~59 I.U./ml of GDH. The assay was visualized with a standard DAPI filter set (Nikon). When released, glutamate is converted by GDH to α-ketoglutarate, while bath supplied NAD^+ is reduced to NADH, a fluorescent product when excited by UV light. The fluorescence trace of the experimental run was subtracted from that obtained during the sham run. We analyzed regions of interest near solitary astrocytes since they are devoid of intracellular NADH signal, and thus record extracellular NADH fluorescence which reports on released glutamate. Fluorescence data was expressed as dF/Fo (%) with the baseline fluorescence (Fo) being the fluorescence of the media surrounding the astrocyte before mechanical stimulation.

Cell transfection

Transfection was done using purified astrocytes and transfection reagent (TransIT-293, Mirus) as we described in detail elsewhere (Malarkey and Parpura, 2011). Briefly, co-complexes of the plasmids (each at 0.5 μg) encoding vesicular glutamate transporter 3 (VGLUT3) appended at its C-terminus with enhanced green fluorescent protein (VGLUT3-EGFP; provided by Dr. Salah El Mestikawy, INSERM U513, Creteil Cedex, France) and monomeric Red Fluorescent Protein [mRFP, provided by Dr. Gyorgy Hajnóczky, Thomas Jefferson University, Philadelphia, PA, USA (Csordas et al., 2006)] were transiently applied (3 hours) to Petri dishes (35 mm in diameter) containing astrocyte cultures grown on PEI-coated coverslips. Astrocytes were imaged 3 days post-transfection.

Image acquisition and processing

For calcium and glutamate imaging an inverted microscope (TE 300, Nikon, Melville, NY) was used, along with image processing, as described previously (Reyes et al., 2011). Briefly, cumulative responses were obtained by summing dF/Fo values for all time points after mechanical stimulation. The peak and cumulative dF/Fo from WT and BACHD were ranked and normalized to WT to accommodate for variations in culture conditions, and to allow comparisons between experimental batches. For Total Internal Reflection Fluorescence Microscopy (TIRFM) imaging we used an inverted microscope (IX81; Olympus, Center Valley, PA) with associated equipment, as reported elsewhere (Kapoor et al., 2011). Analysis of vesicular occupancy of the astrocyte area within TIRF field was done using Metamorph imaging software ver. 6.1 (Molecular Devices, Chicago, IL). To denote the area of an individual astrocyte within the TIRF field, an mRFP image was threshold by 1 standard deviation of fluorescence intensity of the entire image; pixels values exceeding this threshold represented the area of an astrocyte within the TIRF field. This area was transposed onto the corresponding VGLUT3-EGFP image of the cell of interest and number

of VGLUT3-EGFP positive pixels within that area, defined as pixels with fluorescence intensity value above the average fluorescence intensity of the area + 3 standard deviations, were obtained. The proportion of cell area occupied by VGLUT3-laden vesicles was calculated as percentage of positive VGLUT-3 pixels over pixels representing astrocyte area.

Subcellular fractionation

Mitochondria were isolated from astrocytes plated and purified in flasks as we previously described (Reyes et al., 2011); the cytosolic extract was also obtained during this procedure. Astrocytes were disrupted by nitrogen cavitation (1.7 MPa) for 10 min on ice. Cell lysate was centrifuged at 50 × g for 10 min at 4°C and supernatant centrifuged at 1000 x g for 10 min at 4°C. Crude cytosolic fraction was obtained by centrifugation of the 1000 × g supernatant at 20000 × g for 10 min at 4°C; resulting supernatant was used as a cytosolic fraction. To purify mitochondria, the 1000 × g pellet was resuspended in cavitation buffer containing protease inhibitors and layered over a discontinuous 1.0/1.5 M sucrose gradient prior to centrifuging for 1 h at 80000 × g in a swinging bucket rotor at 4°C. Mitochondrial fraction was recovered from the interface and diluted 1:2 in 5 mM HEPES (pH 7.4), 3 mM $MgCl_2$ and 1 mM EGTA prior to centrifugation at 20000 × g for 20 min. The resulting pellet was resuspended in cavitation buffer, washed two times by centrifugation at 6800 × g for 5 min with the resulting pellet containing the purified mitochondria. We obtained non-nuclear membrane and vesicle extracts from cultured astrocytes, as described previously (Parpura et al., 1995), for analysis of VGLUT3.

Western blotting

Total protein was extracted from purified and cultured (2-3 weeks) astrocytes from WT and BACHD mice using RIPA buffer. Subcellular fractionation samples above were also used for Western blotting. Protein samples were prepared for loading by heating in NuPAGE LDS buffer (Invitrogen) for 10 min at 70°C, resolved on 3–8% Tris-acetate NuPAGE gels (Invitrogen) using Tris-acetate running buffer, and then wet-transferred onto PVDF membranes using NuPAGE transfer buffer (Invitrogen). Immunoblots were probed with antibodies against huntingtin (2166, 1:3000 or 1C2, 1:3000 Millipore), α-tubulin (1:3000, Sigma-Aldrich), succinate dehydrogenase/complex II 70 kDa subunit (1:5000, Invitrogen), pyruvate carboxylase (1:3000, Novus Biologicals), glutamine synthetase (1:1000, Millipore), vesicular glutamate transporter 3 (1:5000, Chemicon, presently available through Millipore) and β-actin (1:3000, Sigma-Aldrich) in 5% blocking solution. Chemiluminescent detection was accomplished using SuperSignal West Pico Chemiluminescent Substrate reagents (Thermo Scientific).

Statistical analysis

The comparisons between WT and BACHD data on cytosolic Ca^{2+} dynamics, exocytotic glutamate release, cellular area occupied by VGLUT3, and protein levels were done using Mann-Whitney U-test. Wilcoxon signed-rank test was used to compare peak and cumulative glutamate release in BACHD astrocytes.

Results

Mutant huntingtin expression in BACHD astrocytes

The BACHD mouse model expresses full-length human mhtt throughout the brain. These mice exhibit progressive motor dysfunction, psychiatric-like disturbances, and neuropathological changes including mhtt aggregation (Gray et al., 2008; Menalled et al., 2009). While studies on astrocytes in R6/2 mice (Shin et al., 2005) are enormously

informative, this model expresses only a small fragment of the mutant protein. A model that expresses full-length mutant huntingtin (fl-mhtt) and reproduces many aspects of the disorder is likely a more relevant model that may provide additional insight into HD pathogenesis that is not due to mhtt fragmentation (Gray et al., 2008). While htt is expressed throughout the brain in various cell types, we assessed the expression of the htt protein in cultured astrocytes from BACHD mice. We prepared cultures of purified cortical astrocytes from BACHD and WT mouse pups. Indirect ICC of the astrocyte specific marker GFAP shows similar labeling in both WT and BACHD cells (Figure 1 A, top panel, WT; bottom panel, BACHD respectively). Based on counterstaining the cell nuclei with DAPI, both WT and BACHD cultures were highly purified for astrocytes (>99%); all nuclei were associated with the positive immunoreactivity for GFAP in WT (n=154 of 154 tested) and BACHD (n=141 of 141 tested) cultures (Figure 1A; merged images).

While mhtt has been seen in astrocytes in HD patient tissue (Singhrao et al., 1998), and aggregated mhtt has been seen in other mouse models of HD (Bradford et al., 2010), the presence of the protein in BACHD astrocytes has not been determined to date. We confirmed the presence of htt in purified astrocytes from WT and BACHD purified astrocytes. Western blots using the mAb2166 antibody revealed the presence of endogenous mouse htt in WT and BACHD astrocytes. Additionally, the human mhtt protein was present in BACHD astrocytes (Figure 1C) as revealed by the monoclonal antibody 2166, which recognizes both endogenous mouse (lower band) and human mhtt (upper band) proteins. The expanded ft-mhtt protein was identified in BACHD astrocytes with the monoclonal antibody 1C2 that recognizes htt with expanded polyglutamines. The level of endogenous mouse htt protein was equal between WT and BACHD astrocytes, while the mhtt level was slightly less than endogenous mouse htt in the BACHD astrocytes. Having determined the expression of (m)htt in our cultured astrocytes, we next studied what effect fl-mhtt in BACHD astrocytes had on their ability to release glutamate by exocytosis.

Enhanced Ca^{2+}-dependent exocytotic release of glutamate from BACHD astrocytes

Excessive activation of glutamate receptors leading to excitotoxicity is one of the implicated toxic mechanisms in HD. However, the cellular source of glutamate and the underlying mechanism(s) of its increased extracellular levels contributing to excitotoxicity in HD remain unclear. Here, using BACHD mice (Gray et al., 2008) we test the possibility that exocytosis of glutamate by astrocytes could be a source of the excitotoxic drive. It should be noted that astrocytes can release glutamate utilizing various mechanisms (Malarkey and Parpura, 2008). However, mechanical stimulation assesses the exocytotic/vesicular release of glutamate, as evidenced by its exquisite sensitivity (97%) to a pharmacological blocker of VGLUTs (Montana et al., 2004). Consequently, using solitary astrocytes from purified cultures of WT and BACHD mice we compared their ability to respond to mechanical stimulation by an increase in cytosolic Ca^{2+} (Ca^{2+}_{cyt}) levels and consequential exocytotic glutamate release. Solitary astrocytes were used to decrease the likelihood of communication amongst astrocytes, which could otherwise affect our measurements (Lee et al., 2008; Montana et al., 2004).

In order to examine Ca^{2+}_{cyt} responses, astrocytes from WT and BACHD cultures were loaded with the fluorescent Ca^{2+} indicator fluo-3. As expected, mechanical stimulus caused a typical increase in Ca^{2+}_{cyt} levels in solitary astrocytes characterized by an initial transient Ca^{2+} elevation followed by a slow decay (Figure 2A). Two aspects of the Ca^{2+}_{cyt} kinetics in astrocytes were measured and analyzed: the peak and cumulative Ca^{2+} responses (Figure 2B and C, respectively). The peak response represents the maximum Ca^{2+}_{cyt} in the stimulated astrocyte as a result of Ca^{2+} entry into the cytosol from the endoplasmic reticulum (ER) store and the extracellular space (ECS), while the cumulative response additionally represents the declining Ca^{2+}_{cyt} as free Ca^{2+} is extruded from the cytosol by

the plasma membrane and ER Ca^{2+} pumps (Hua et al., 2004; Reyes et al., 2012). Mitochondria modulate the peak of Ca^{2+}_{cyt} transient as they immediately sequester Ca^{2+}, while during the decay phase they slowly release Ca^{2+} (Reyes and Parpura, 2008; Reyes et al., 2011). Our analysis of the Ca^{2+}_{cyt} dynamics reveals no significant differences between WT and BACHD astrocytes in peak and cumulative values (Figure 2B and C, respectively; n=19 for both groups; Mann-Whitney U-test, p=0.76 for both comparisons). These data suggest that the presence of fl-mhtt protein in astrocytes does not alter global Ca^{2+}_{cyt} dynamics in response to mechanical stimulation.

To study mechanically-induced Ca^{2+}-dependent exocytotic glutamate release from WT and BACHD solitary astrocytes, we optically monitored glutamate released into the ECS surrounding cultured astrocytes using an enzyme-linked assay based on accumulation of the fluorescent product NADH (Montana et al., 2004). Mechanical stimulation of WT astrocytes caused glutamate release as indicated by a transient increase in NADH fluorescence, reporting on extracellular glutamate levels (Figure 2D). Surprisingly, while BACHD astrocytes showed similar Ca^{2+}_{cyt} dynamics to those of WT astrocytes, in BACHD astrocytes there was a robust enhancement of the ability to release glutamate into the ECS, as seen by a significant increase in the peak and cumulative values (Figure 2E and F, respectively; n=17 for both groups, Mann-Whitney U-test, $p<0.01$ for both comparisons).

Previous work has shown that in normal astrocytes Ca^{2+}-dependent exocytotic release of glutamate from astrocytes has a proportionate relationship to Ca^{2+}_{cyt} responses (Parpura and Haydon, 2000), which can be modulated by various regulatory factors (Ni and Parpura, 2009; Reyes et al., 2011). Thus, the observed augmented (disproportional to Ca^{2+}_{cyt} dynamics) glutamate release from BACHD astrocytes may indicate that mhtt could affect other known limiting factors in regulation of the Ca^{2+}-dependent release of glutamate from astrocytes, including VGLUT3 and the cytosolic concentration of glutamate (Ni and Parpura, 2009).

BACHD astrocytes have increased *de novo* synthesis of glutamate, with no change in glutamine synthetase and vesicular glutamate transporter 3 levels

It has been demonstrated that increased expression of VGLUT3 and the inhibition of glutamine synthetase (GS) activity, which leads to increased cytosolic glutamate concentration, greatly increased mechanically-induced Ca^{2+}- dependent glutamate release from solitary astrocytes, without affecting their Ca^{2+}_{cyt} dynamics (Ni and Parpura, 2009).

Two enzymes, pyruvate carboxylase (PC) and GS, are critical for controlling the level of cytosolic glutamate within astrocytes (Figure 3A). In the brain, glutamate is synthesized *de novo* within astrocytes as a by-product of the tricarboxylic acid cycle (Hertz et al., 1999) owing to glucose, i.e. pyruvate, entry into this cycle via PC. Once in the cytosol, glutamate can then be concentrated in vesicles mainly by VGLUT3 (Ni and Parpura, 2009) or converted to glutamine by GS.

Since it has been shown that mhtt can affect axonal traffic in neurons, including mitochondrial (Trushina et al., 2004) and vesicular trafficking (Gauthier et al., 2004), mhtt expression in BACHD astrocytes could lead to a differential accumulation of VGLUT3-laden vesicles at sites of exocytosis at/near the plasma membrane and thus result in increased glutamate release. To address this, we used TIRFM, which provides an excellent method for studying fluorescently tagged molecules at and/or very near to the plasma membrane in live cells (Kapoor et al., 2011; Malarkey and Parpura, 2011). We co-transfected astrocytes using plasmids to express VGLUT3-EGFP along with the co-transfection marker mRFP, that localizes in the cytosol. For each solitary astrocyte, we acquired matching images of mRFP and VGLUT3-EGFP. As expected from TIRF

visualization of the thin layer of the cytosol above the plasma membrane attached to the glass coverslip (penetration depth of the TIRF illumination was ~ 80 nm from the glass coverslip), mRFP showed a diffuse stain, which was used to define the total cellular area attached to the glass coverslip (Figure 3B). VGLUT3-EGFP, characteristically for vesicular proteins, showed a punctate pattern of expression representing vesicles at/very near the plasma membrane (Figure 3C); these vesicles we consider “docked” based on their presence within the TIRF field. We quantified the proportion of the astrocyte area (defined by mRFP) that is occupied by docked VGLUT3-laden vesicles (Figure 3D). In WT astrocytes (n=25) VGLUT3-EGFP stain occupied 1.52 ± 0.11 % of the cell area witting TIRF field. A similar value was obtained from BACHD astrocytes (1.56 ± 0.11 %; n= 26; Mann-Whitney U-test, p=0.73).

We also analyzed VGLUT3 protein levels in cultured astrocytes. We subjected proteins of non-nuclear membrane and vesicle extracts from WT and BACHD astrocytes to Western blot analysis. We found similar expression of VGLUT3 in both types of astrocytes (Figure 3E; n=3, Mann-Whitney U-test, p=0.2). Thus, it appears that mhtt affects neither the proportion of docked VGLUT3 vesicles nor the level of VGLUT3 protein in BACHD cells.

We further examined the molecules involved in controlling glutamate levels within astrocytes using Western blotting. We first examined the level of GS in total cell extracts and found no significant difference between WT and BACHD astrocytes (Figure 4A and B; n=4, Mann-Whitney U-test, p=0.3). We next performed subcellular fractionation to isolate mitochondria, extracted mitochondrial protein and performed Western blots. We found a significant increase in the level of PC in mitochondria from BACHD astrocytes when compared to WT (Figure 4C and D; n=4, Mann-Whitney U-test, $p<0.03$). Taken together, this result indicates that cultured BACHD astrocytes have an increased expression of PC, which can lead to the generation of more cytosolic glutamate. Due to this increased availability of glutamate, VGLUT3 fills vesicles with this transmitter to a greater extent in BACHD astrocytes than in WT astrocytes. Consequently, BACHD astrocytes show an augmented exocytotic release of glutamate when compared to WT astrocytes in spite of preserved Ca^{2+} dynamics. These data identify a novel cell-autonomous effect of mhtt on BACHD astrocytes, which in the context of the intact nervous system could have deleterious affects on the proper function of neural circuits/networks.

Discussion

We identify here a new cell autonomous astrocyte phenotype in an HD model. This phenotype appears to arise from an increase in the level of PC and increased astrocytic glutamate synthesis that causes an augmentation of exocytotic release of glutamate from these cells into the ECS.

There are multiple experiments to support mhtt causing Ca^{2+} handling deficits and decreased mitochondrial ATP production (Lodi et al., 2000; Panov et al., 2002). Mitochondrial dysfunction in HD patients is indicated by severe weight loss and muscle wasting despite constant and increased food intake (Djousse et al., 2002), and changes in glucose and lactate metabolism indicative of a bioenergetic deficit (Jenkins et al., 1998). However, our data on mechanically-induced cytosolic Ca^{2+} levels does not reveal any apparent differences in mitochondrial Ca^{2+} buffering between cultured BACHD and WT cortical astrocytes. It is possible that this result is consequential to a compensatory action occurring at the level of the ER and/or the plasma membrane as they contain additional molecular entities regulating cytosolic Ca^{2+} dynamics in astrocytes (Parpura et al., 2011). Such compensatory events may mask expected defects in mitochondrial Ca^{2+} buffering in BACHD astrocytes. The future work detailing this possible scenario would need to include a

battery of pharmacological and molecular biology/genetics approaches already implemented in this branch of astroglial research (Parnis et al., 2013; Reyes and Parpura, 2008; Reyes et al., 2011).

Vesicular and mitochondrial trafficking in neurons is affected by mhtt (Bossy-Wetzel et al., 2008; Gauthier et al., 2004; Truant et al., 2006). Based on VGLUT3-EGFP data we find no evidence for mhtt affecting docking of VGLUT3-laden vesicles in astrocytes. However, it is possible that in astrocytes *in vivo*, where they have more elaborate processes, there could be an impairment of mitochondrial and/or vesicular trafficking to more distal processes. If so, mitochondria and perhaps VGLUT3 vesicles would be located more proximally towards astrocytic cell bodies and away from synaptic sites. In the scenario where only mitochondrial, but not vesicular trafficking would be affected, there would be a cytosolic glutamate gradient with lower concentrations towards peripheral processes, where VGLUT3 vesicles would poorly fill. In contrast, VGLUT3 vesicles located within astrocytic cell bodies and proximal processes would be inundated with heightened cytosolic glutamate and well loaded. Since astrocytes can release glutamate by exocytosis from both their cell bodies and processes [reviewed in (Montana et al., 2006)] in either of the above scenarios they could differentially release augmented loads of glutamate at neuronal extrasynaptic sites.

We identify an increase in PC levels in BACHD astrocytes. It remains to be determined if this increase in PC levels is due to transcriptional dysregulation or protein stability in these cells. While we conclude that this increase in PC is the likely cause of increased glutamate release from these cells, it should be noted, however, that mhtt effect on the enhancement of glutamate release could be in part attributed to the expected impairment of glutamate uptake (Behrens et al., 2002; Lievens et al., 2001). To contemplate such a possible scenario three findings/deductions need to be considered. i) Mechanical stimulation (within 3-6 s of the onset) causes an exocytotic burst (Malarkey and Parpura, 2011), characterized by an initial transient and high rate of vesicular fusions, followed by a slow and sustained rate of fusions. The normalized peak of glutamate release therefore represents the exocytotic burst, while the follow-up low rate sustained vesicular fusions contribute to the vast majority of normalized cumulative glutamate release. ii) Mechanical stimulation leads not only to fast Ca^{2+} (on average reached peak 4-6 s after initiation of the stimulus), but also to delayed Na^{+} cytosolic loads (on average reached peak 20-32 s after initiation of the stimulus) (Reyes et al., 2012); increased Na^{+} cytosolic slows down operation of EAATs due to reduced ion gradient (Kirischuk et al., 2012). iii) Since the Ca^{2+}-dependent exocytosis in astrocytes results in release with localized extracellular glutamate accumulation of 1-100 μM (Innocenti et al., 2000), with concomitant glutamate removal by EAATs [K_m ~ 20 μM; for details see (Danbolt, 2001)], a possible contribution of EAATs in mechanically-induced glutamate release would be more prominent in the cumulative than the peak parameter. Consequently, in support of the notion that BACHD astrocytes might have reduced levels of EAATs, we have observed some discrepancy between normalized peak vs. cumulative glutamate release in these cells. Mechanically induced cumulative release was more augmented (median value of ~2.1 times over WT) than the peak (median value of ~1.6 times over WT) release, albeit this difference was statistically insignificant (Wilcoxon signed-rank test, p=0.1). Furthermore, the increase in the cumulative glutamate release was lesser than expected from the increase in PC levels in BACHD astrocytes (median value of ~ 2.9 over WT). Thus, a possible reduction of glutamate uptake in BACHD astrocytes could only be a minor contributor to the enhancement of mechanically induced exocytotic glutamate release. Additional modulation of glutamate release augmentation in BACHD astrocytes could originate from changes that might occur in the metabolic pathway between PC and GS. This hypothetical scenario could involve various mitochondrial enzymes, such as the previously mentioned AAT (Figure 3A), and/or solute carriers (SLC) redistributing reactants/products across the inner mitochondrial membrane, such as mitochondrial glutamate carrier 1 (SLC

family 25 member 22) and mitochondrial aspartate glutamate carrier (SLC family 25 member 13, also called citrin).

Glutamate released from astrocytes by exocytosis can act on neuronal extrasynaptic NMDARs to modulate neuronal excitability and synaptic transmission (Fellin et al., 2004). NMDARs may have different roles depending on whether they are present in synaptic or extrasynaptic sites. When present at the synapse, these receptors activate cell survival pathways, while extrasynaptically located receptors activate pathways that lead to cell death (Papadia and Hardingham, 2007). Interestingly, an imbalance between synaptic and extrasynaptic NMDAR activity has been observed in the YAC128 mouse model of HD. In this model there was an increase in current due to extrasynaptic NMDARs in striatal MSNs (Milnerwood and Raymond, 2007). It has been hypothesized that the activation of these extrasynaptic NMDARs in HD is due to glutamate spillover from the synapse. However, it is not yet clear where the glutamate required for this activation is sourced and why there is more of it in HD. While it is possible that a lack of clearance by the plasma membrane glutamate transporters could contribute to more activity at extrasynaptic sites [which incidentally have much lower density of glial EAATs than perisynaptic sites (Danbolt, 2001)], however, based on the data presented here, we suggest the possibility that glutamate derived and exocytotically released from astrocytes may be acting on these extrasynaptic NMDA receptors and contributing to cell death. Although, this work does not address striatal astrocytes, it indeed provides an interesting finding that may also be applicable to mhtt expressing striatal astrocytes. Nonetheless, this novel phenotype raises the possibility that not only the compromised ability of astrocytes to uptake glutamate (Behrens et al., 2002; Lievens et al., 2001), but also their increased capability to exocytotically release this transmitter could lead to excessive amounts of glutamate in the ECS and contribute to excitotoxicity in HD.

Acknowledgments

This work was supported by the National Institutes of Health NINDS (K01NS069614), Dixon Family Foundation to M.G. and the National Science Foundation (CBET 0943343) to V.P.

References

Albin RL, et al. Preferential loss of striato-external pallidal projection neurons in presymptomatic Huntington's disease. Ann Neurol. 1992; 31:425–30. [PubMed: 1375014]

Araque A, et al. Tripartite synapses: glia, the unacknowledged partner. Trends Neurosci. 1999; 22:208–15. [PubMed: 10322493]

Arzberger T, et al. Changes of NMDA receptor subunit (NR1, NR2B) and glutamate transporter (GLT1) mRNA expression in Huntington's disease--an in situ hybridization study. J Neuropathol Exp Neurol. 1997; 56:440–54. [PubMed: 9100675]

Beal MF, et al. Replication of the neurochemical characteristics of Huntington's disease by quinolinic acid. Nature. 1986; 321:168–71. [PubMed: 2422561]

Behrens PF, et al. Impaired glutamate transport and glutamate-glutamine cycling: downstream effects of the Huntington mutation. Brain. 2002; 125:1908–22. [PubMed: 12135980]

Bossy-Wetzel E, et al. Mutant huntingtin and mitochondrial dysfunction. Trends Neurosci. 2008; 31:609–16. [PubMed: 18951640]

Bradford J, et al. Mutant huntingtin in glial cells exacerbates neurological symptoms of Huntington disease mice. J Biol Chem. 2010; 285:10653–61. [PubMed: 20145253]

Csordas G, et al. Structural and functional features and significance of the physical linkage between ER and mitochondria. J Cell Biol. 2006; 174:915–21. [PubMed: 16982799]

Danbolt NC. Glutamate uptake. Prog Neurobiol. 2001; 65:1–105. [PubMed: 11369436]

Djousse L, et al. Weight loss in early stage of Huntington's disease. Neurology. 2002; 59:1325–30. [PubMed: 12427878]

Faideau M, et al. In vivo expression of polyglutamine-expanded huntingtin by mouse striatal astrocytes impairs glutamate transport: a correlation with Huntington's disease subjects. Hum Mol Genet. 2010; 19:3053–67. [PubMed: 20494921]

Fan MM, Raymond LA. N-methyl-D-aspartate (NMDA) receptor function and excitotoxicity in Huntington's disease. Prog Neurobiol. 2007; 81:272–93. [PubMed: 17188796]

Fellin T, et al. Neuronal synchrony mediated by astrocytic glutamate through activation of extrasynaptic NMDA receptors. Neuron. 2004; 43:729–43. [PubMed: 15339653]

Gauthier LR, et al. Huntingtin controls neurotrophic support and survival of neurons by enhancing BDNF vesicular transport along microtubules. Cell. 2004; 118:127–38. [PubMed: 15242649]

Gottipati MK, et al. Chemically functionalized water-soluble single-walled carbon nanotubes modulate morpho-functional characteristics of astrocytes. Nano Lett. 2012; 12:4742–7. [PubMed: 22924813]

Gray M, et al. Full-length human mutant huntingtin with a stable polyglutamine repeat can elicit progressive and selective neuropathogenesis in BACHD mice. J Neurosci. 2008; 28:6182–95. [PubMed: 18550760]

Group, H. s. D. C. R. A novel gene containing a trinucleotide repeat that is expanded and unstable on Huntington's disease chromosomes. Cell. 1993; 72:971–83. [PubMed: 8458085]

Gu X, et al. Pathological cell-cell interactions are necessary for striatal pathogenesis in a conditional mouse model of Huntington's disease. Mol Neurodegener. 2007; 2:8. [PubMed: 17470275]

Gu X, et al. Pathological cell-cell interactions elicited by a neuropathogenic form of mutant Huntingtin contribute to cortical pathogenesis in HD mice. Neuron. 2005; 46:433–44. [PubMed: 15882643]

Hassel B, et al. Glutamate uptake is reduced in prefrontal cortex in Huntington's disease. Neurochem Res. 2008; 33:232–7. [PubMed: 17726644]

Hedreen JC, et al. Neuronal loss in layers V and VI of cerebral cortex in Huntington's disease. Neurosci Lett. 1991; 133:257–61. [PubMed: 1840078]

Hertz L, et al. Astrocytes: glutamate producers for neurons. J Neurosci Res. 1999; 57:417–28. [PubMed: 10440891]

Hua X, et al. Ca2+-dependent glutamate release involves two classes of endoplasmic reticulum Ca2+ stores in astrocytes. J Neurosci Res. 2004; 76:86–97. [PubMed: 15048932]

Innocenti B, et al. Imaging extracellular waves of glutamate during calcium signaling in cultured astrocytes. J Neurosci. 2000; 20:1800–8. [PubMed: 10684881]

Jenkins BG, et al. 1H NMR spectroscopy studies of Huntington's disease: correlations with CAG repeat numbers. Neurology. 1998; 50:1357–65. [PubMed: 9595987]

Kapoor N, et al. Interaction of ASIC1 and ENaC subunits in human glioma cells and rat astrocytes. Am J Physiol Cell Physiol. 2011; 300:C1246–59. [PubMed: 21346156]

Kirischuk S, et al. Sodium dynamics: another key to astroglial excitability? Trends Neurosci. 2012

Landwehrmeyer GB, et al. NMDA receptor subunit mRNA expression by projection neurons and interneurons in rat striatum. J Neurosci. 1995; 15:5297–307. [PubMed: 7623152]

Lee W, et al. Micropit: A New Cell Culturing Approach for Characterization of Solitary Astrocytes and Small Networks of these Glial Cells. Front Neuroeng. 2008; 1:2. [PubMed: 19129909]

Lievens JC, et al. Impaired glutamate uptake in the R6 Huntington's disease transgenic mice. Neurobiol Dis. 2001; 8:807–21. [PubMed: 11592850]

Lodi R, et al. Abnormal in vivo skeletal muscle energy metabolism in Huntington's disease and dentatorubropallidoluysian atrophy. Ann Neurol. 2000; 48:72–6. [PubMed: 10894218]

Malarkey EB, Parpura V. Mechanisms of glutamate release from astrocytes. Neurochem Int. 2008; 52:142–54. [PubMed: 17669556]

Malarkey EB, Parpura V. Temporal characteristics of vesicular fusion in astrocytes: examination of synaptobrevin 2-laden vesicles at single vesicle resolution. J Physiol. 2011; 589:4271–300. [PubMed: 21746780]

Maragakis NJ, Rothstein JD. Glutamate transporters in neurologic disease. Arch Neurol. 2001; 58:365–70. [PubMed: 11255439]

Menalled L, et al. Systematic behavioral evaluation of Huntington's disease transgenic and knock-in mouse models. Neurobiol Dis. 2009; 35:319–36. [PubMed: 19464370]

Milnerwood AJ, Raymond LA. Corticostriatal synaptic function in mouse models of Huntington's disease: early effects of huntingtin repeat length and protein load. J Physiol. 2007; 585:817–31. [PubMed: 17947312]

Montana V, et al. Vesicular transmitter release from astrocytes. Glia. 2006; 54:700–15. [PubMed: 17006898]

Montana V, et al. Vesicular glutamate transporter-dependent glutamate release from astrocytes. J Neurosci. 2004; 24:2633–42. [PubMed: 15028755]

Ni Y, Parpura V. Dual regulation of Ca2+-dependent glutamate release from astrocytes: vesicular glutamate transporters and cytosolic glutamate levels. Glia. 2009; 57:1296–305. [PubMed: 19191347]

Panov AV, et al. Early mitochondrial calcium defects in Huntington's disease are a direct effect of polyglutamines. Nat Neurosci. 2002; 5:731–6. [PubMed: 12089530]

Papadia S, Hardingham GE. The dichotomy of NMDA receptor signaling. Neuroscientist. 2007; 13:572–9. [PubMed: 18000068]

Parnis J, et al. Mitochondrial Exchanger NCLX Plays a Major Role in the Intracellular Ca2+ Signaling, Gliotransmission, and Proliferation of Astrocytes. J Neurosci. 2013; 33:7206–19. [PubMed: 23616530]

Parpura V, et al. Expression of synaptobrevin II, cellubrevin and syntaxin but not SNAP-25 in cultured astrocytes. FEBS Lett. 1995; 377:489–92. [PubMed: 8549782]

Parpura V, et al. Ca2+ sources for the exocytotic release of glutamate from astrocytes. Biochim Biophys Acta. 2011; 1813:984–91. [PubMed: 21118669]

Parpura V, Haydon PG. Physiological astrocytic calcium levels stimulate glutamate release to modulate adjacent neurons. Proc Natl Acad Sci U S A. 2000; 97:8629–34. [PubMed: 10900020]

Parpura V, Zorec R. Gliotransmission: Exocytotic release from astrocytes. Brain Res Rev. 2010; 63:83–92. [PubMed: 19948188]

Reyes RC, Parpura V. Mitochondria modulate Ca2+-dependent glutamate release from rat cortical astrocytes. J Neurosci. 2008; 28:9682–91. [PubMed: 18815254]

Reyes RC, et al. Immunophilin deficiency augments Ca2+-dependent glutamate release from mouse cortical astrocytes. Cell Calcium. 2011; 49:23–34. [PubMed: 21163525]

Reyes RC, et al. Plasmalemmal Na+/Ca2+ exchanger modulates Ca2+-dependent exocytotic release of glutamate from rat cortical astrocytes. ASN Neuro. 2012; 4:pii: e00075. doi: 10.1042/AN20110059.

Sharp AH, et al. Widespread expression of Huntington's disease gene (IT15) protein product. Neuron. 1995; 14:1065–74. [PubMed: 7748554]

Shin JY, et al. Expression of mutant huntingtin in glial cells contributes to neuronal excitotoxicity. J Cell Biol. 2005; 171:1001–12. [PubMed: 16365166]

Singhrao SK, et al. Huntingtin Protein Colocalizes with Lesions of Neurodegenerative Diseases: An Investigation in Huntington's, Alzheimer's, and Pick's Diseases. Experimental Neurology. 1998; 150:213–222. [PubMed: 9527890]

Truant R, et al. Hypothesis: Huntingtin may function in membrane association and vesicular trafficking. Biochem Cell Biol. 2006; 84:912–7. [PubMed: 17215878]

Trushina E, et al. Mutant huntingtin impairs axonal trafficking in mammalian neurons in vivo and in vitro. Mol Cell Biol. 2004; 24:8195–209. [PubMed: 15340079]

Vonsattel JP, DiFiglia M. Huntington disease. J Neuropathol Exp Neurol. 1998; 57:369–84. [PubMed: 9596408]

Vonsattel JP, et al. Neuropathological classification of Huntington's disease. J Neuropathol Exp Neurol. 1985; 44:559–77. [PubMed: 2932539]

Highlights

- Mutant huntingtin affects levels of glutamate released from cultured astrocytes.
- There is no change in vesicular glutamate transporter 3 trafficking in mhtt astrocytes.
- Glutamine synthetase levels are normal in cultured mhtt astrocytes.
- Elevated pyruvate carboxylase in mhtt astrocytes could lead to increased glutamate.

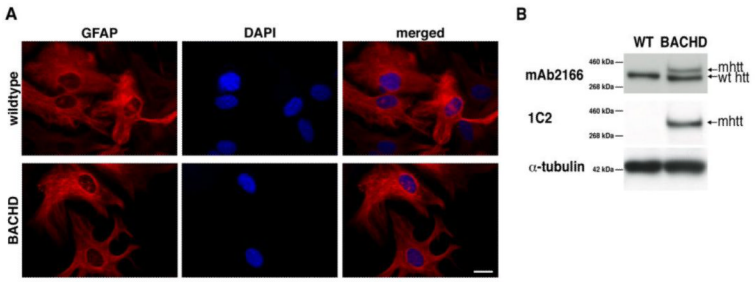

Figure 1. Huntingtin expression in cultured WT and BACHD astrocytes

(A) GFAP immunocytochemistry on purified WT and BACHD astrocytes, whose nuclei are counterstained with DAPI. Both WT and BACHD cultured astrocytes show similar GFAP stain. Scale bar, 20μm. (B) Western blot analysis of protein extracted from cultured astrocytes with the monoclonal antibody 2166 (top panel) that stains endogenous mouse htt and full-length human mhtt in BACHD astrocytes. Only the endogenous mouse protein is found in WT mice, while both endogenous and full-length human mhtt are seen in the BACHD lane. The monoclonal antibody 1C2 (middle panel) recognizes an expanded polyQ epitope and reveals full-length human mhtt in BACHD astrocytes and no bands in WT. Immunoreactivity of α-tubulin was used as a control for gel loading (bottom panel).

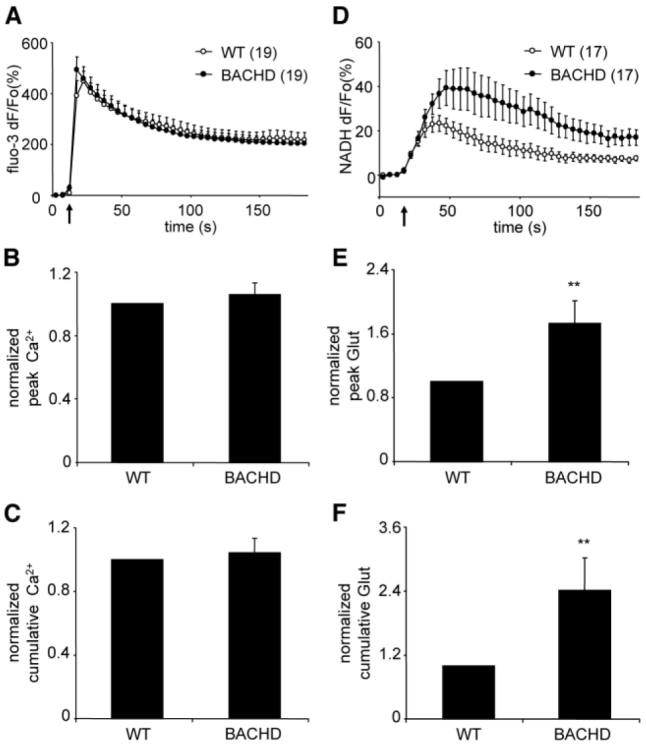

Figure 2. Cultured cortical astrocytes from BACHD mice exhibit the same cytosolic Ca^{2+} responses, but augmented glutamate release in response to mechanical stimulation when compared to cortical astrocytes from WT mice

(A) Average kinetics of the fluo-3 fluorescence indicating the change in cytosolic Ca^{2+}. (B) Normalized fluo-3 peak fluorescence values of mechanically-stimulated astrocytes. (C) Normalized fluo-3 cumulative fluorescence values obtained from mechanically-stimulated astrocytes. (D) Average kinetics of the NADH fluorescence reporting on glutamate released by astrocytes. (E-F) Normalized peak (E) and cumulative (F) glutamate (Glut) release from mechanically-stimulated astrocytes. BACHD astrocytes display significantly higher peak and cumulative glutamate release than WT control astrocytes. Points and bars represent means ± SEMs of measurements from solitary astrocytes (numbers for A-C and D-F listed in parentheses of A and D, respectively) expressed as dF/Fo (percentage) or normalized (ratio to control), while arrows (in A and D) represent the time when mechanical stimulation was applied to the cells. Asterisks denote significant change in comparison to control (WT) group (Mann-Whitney U-test, **$p<0.01$).

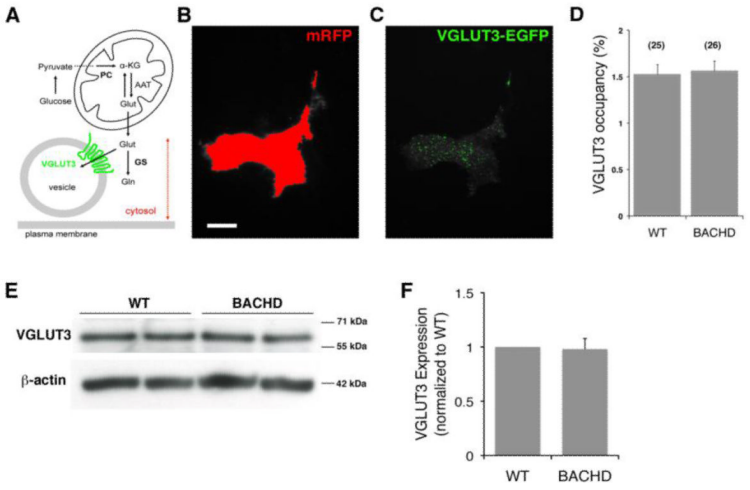

Figure 3. Vesicular glutamate transporter 3 (VGLUT3) levels are unaltered in BACHD astrocytes

(A) Schematic representing regulation of glutamate in exocytotic glutamate release from astrocytes. Glutamate (Glut) can be synthesized in astrocytes *de novo* from glucose entry through the tricarboxylic acid cycle via pyruvate carboxylase (PC); glucose is broken down to pyruvate in the cytosol. Glutamate is converted from the cycle intermediate, α-ketoglutarate (α-KG), usually by transamination of aspartate *via* mitochondrial aspartate amino transferase (AAT). The synthesized glutamate once in the cytosol can then be converted to glutamine (Gln) by glutamine synthetase (GS), or transported into vesicles via vesicular glutamate transporters (VGLUTs), especially isoform 3 (VGLUT3). Drawing is not to scale. Dotted double arrow denotes intracellular penetration depth of total internal refection fluorescence (TIRF) illumination (~ 80 nm from the glass coverslip) used in experiments in B-D. (B-C) TIRF images of a WT astrocyte co-expressing mRFP (B) and VGLUT3-EGFP (C). (B) To designate the area within the TIRF field of an individual astrocyte, a threshold was applied to mRFP fluorescence emission (red). (C) This area was transposed on the VGLUT3-EGFP image, and VGLUT3-EGFP positive coverage was recorded (green). Scale bar in B, 20 μm. (D) The proportion of the cell area occupied by VGLUT3-laden vesicles (%) was similar in WT and BACHD astrocytes. Bars represent means ± SEMs of measurements from individual solitary astrocytes (numbers listed in parentheses). (E) Representative Western blots probing VGLUT3 from WT and BACHD astrocytes. Immunoreactivity of β-actin was used as a control for gel loading (bottom panel). (F) Quantification of Western blots shows no significant change in the level of VGLUT3 levels between WT and BACHD (n=3).

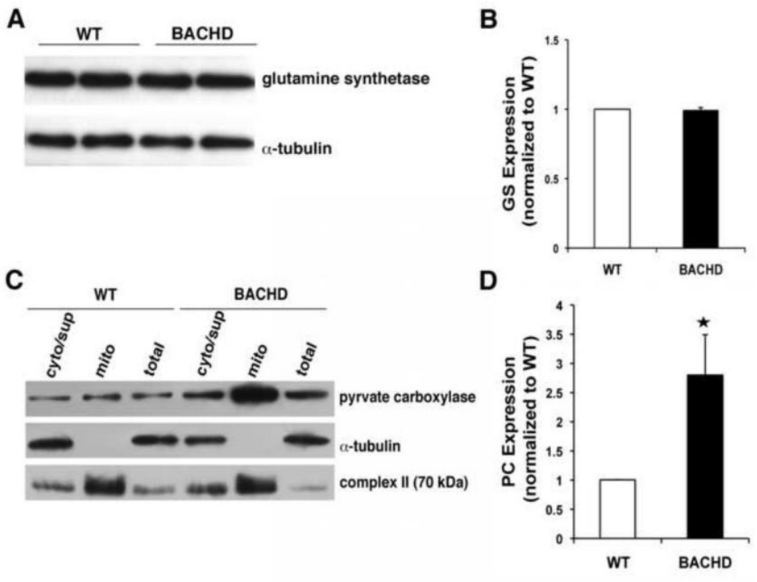

Figure 4. Pyruvate carboxylase expression is increased while glutamine synthetase is unaltered in BACHD astrocytes

(A) Representative Western blot probing glutamine synthetase levels in astrocytes. Immunoreactivity of α-tubulin was used as a control for gel loading. (B) Quantification of glutamine synthetase (GS) levels (n=4) shows no difference between BACHD and WT astrocytes. (C) Representative Western blots of total, cytosolic (i.e. non-mitochondrial supernatant; cyt/sup) and mitochondrial (mito) protein in BACHD and WT astrocytes probing pyruvate carboxylase. Immunoreactivity of cytosolic α-tubulin and mitochondrial complex II were used to confirm success of our fractionation procedure. Note that the aggressive mitochondrial purification (exclusion) approach results in some contamination of the cytosolic/supernatant fraction by mitochondrial proteins. (D) Quantification of pyruvate carboxylase (PC) levels show ~3-fold increase in BACHD mitochondria (n=4 mice, Mann-Whitney U-test, *p <0.03). Data shown as mean ± SEMs.